

## **Electronic Supplementary Information**

### **Facile Synthesis of 1D Organic–Inorganic Perovskite Micro-Belts with High Water Stability for Sensor and Photonic Applications**

**Xiaogang Yang,<sup>ab</sup> Lu-Fang Ma,<sup>b</sup> and Dongpeng Yan<sup>\*a</sup>**

[a] Beijing Key Laboratory of Energy Conversion and Storage Materials, College of Chemistry, Beijing Normal University, Beijing 100875, P. R. China. E-mail: yandp@bnu.edu.cn

[b] College of Chemistry and Chemical Engineering, Henan Province Function-oriented Porous Materials Key Laboratory, Luoyang Normal University, Luoyang 471934, P. R. China.

## A. Experimental Section

### 1. Materials and general procedures.

Analytically pure  $\text{PbCl}_2$ , and acridine (AD) were commercial available, and used without further purification. Single-crystal X-ray diffraction data were collected at room temperature on an Oxford Diffraction SuperNova area-detector diffractometer using mirror optics monochromated  $\text{Mo K}\alpha$  radiation ( $\lambda = 0.71073$  Å). CrysAlisPro<sup>[1]</sup> was used for the data collection, data reduction and empirical absorption correction. The crystal structure was solved by direct methods, using SHELXS-2014 and least-squares refined with SHELXL-2014<sup>[2]</sup> using anisotropic thermal displacement parameters for all non-hydrogen atoms. The crystallographic data for OIHP-AD are listed in Table S1. CCDC No. 1862717 contain the supplementary crystallographic data for OIHP-AD. The data can be obtained free of charge from The Cambridge Crystallographic Data Centre via [http://www.ccdc.cam.ac.uk/data\\_request/cif](http://www.ccdc.cam.ac.uk/data_request/cif). Other data supporting the findings of this study are available from the corresponding author. Powder X-ray diffraction analyses (PXRD) patterns were collected on a Rigaku Ultima-IV automated diffraction system with  $\text{Cu K}\alpha$  radiation ( $\lambda = 1.5406$  Å). Measurements were made in a  $2\theta$  range of  $5\text{--}50^\circ$  at room temperature with a step of  $0.02^\circ$  ( $2\theta$ ) and a counting time of 0.2 s/ step. The operating power was 40 KV, 30 mA. Thermogravimetric analysis (TGA) experiments were carried out using a Perkin-Elmer Diamond SII thermal analyzer from room temperature to  $800^\circ\text{C}$  under a nitrogen atmosphere at a heating rate of  $10^\circ\text{C min}^{-1}$ .

Photographs of the OIHP-AD self-supporting film under UV excitation (365 nm) and ambient conditions were captured using a Canon digital camera (EOS 700D: the ISO value was 400, time of exposure was set to an automatic mode). PL microscope images of OIHP-AD micro-belts were taken under OLYMPUS IXTI fluorescence microscope. The morphology of the samples were investigated by using a scanning electron microscope (SEM Hitachi S-3500) equipped with an energy dispersive X-ray spectrum attachment (EDX Oxford Instruments Isis 300), with an acceleration voltage of 20 kV. Room temperature photoluminescence (PL) spectra and time-resolved lifetime were conducted on an Edinburgh FLS980 fluorescence spectrometer

equipped with a xenon arc lamp (Xe900) and nanosecond flash-lamp (nF900), respectively. The PLQY values at room temperature were estimated using an integrating sphere (F-M101, Edinburgh) accessory in FLS980 fluorescence spectrometer. The temperature dependence of the PL spectra were measured using a temperature controller attached to a cryostat (Oxford Ltd. Optistat DN2) using an FLS980 fluorescence spectrometer. Optical diffuse reflectance spectra were obtained on a Shimadzu UV-3600 spectrophotometer at room temperature. Data were collected in the wavelength range of 200–800 nm. BaSO<sub>4</sub> powder was used as a standard (100% reflectance). Upconversion fluorescence PL spectrum was excited by 800 nm laser on a Tsunami-Spitfire-OPA-800C ultrafast optical parameter amplifier (Spectra Physics). Polarized fluorescence spectrum of the single micro-belt were measured on a CRAIC 508PV microspectrometers ( $\lambda_{\text{ex}} = 420$  nm) by rotating the polarizer at different polarization angle. Spatially resolved PL imaging and spectroscopy of the single micro-belt were taken from a CRAIC 508PV microspectrometers excited by a focused 400 nm laser beam, which was propagated by a optical fiber.

## **2. Preparations of OIHP-AD samples.**

### **2.1 Preparations of OIHP-AD single crystal.**

In a typical synthesis, mixture of AD (0.25 mmol), PbCl<sub>2</sub> (0.5 mmol) and HCl (1 M, 1 mL) were added to water (12 mL) in a 25 mL Teflon-lined stainless steel vessel, and then heated at 120 °C for 12 h. After the reactive mixture was slowly cooled to room temperature, bright yellow belt-like crystals of OIHP-AD were obtained.

### **2.2 Preparations of OIHP-AD micro-belt.**

Addition of a solution of PbCl<sub>2</sub> (0.5 mmol) and HCl (1 M, 0.5 mL) in H<sub>2</sub>O (5 mL) to a solution of AD (0.25 mmol) and HCl (1 M, 0.5 mL) in H<sub>2</sub>O (5 mL) with vigorous string. Then, bright yellow micro-belt crystals of **OIHP-AD** were obtained immediately.

### **2.3 Gram-scale synthesis of OIHP-AD micro-belt.**

Addition of a solution of  $\text{PbCl}_2$  (5 mmol) and  $\text{HCl}$  (1 M, 5 mL) in  $\text{H}_2\text{O}$  (20 mL) to a solution of AD (2.5 mmol) and  $\text{HCl}$  (1 M, 5 mL) in  $\text{H}_2\text{O}$  (20 mL) with vigorous stirring in a vial (50 mL). Then, bright yellow micro-belt crystals of OIHP-AD were obtained immediately.

### 3. Electronic structure calculations of OIHP-AD

All calculations were performed with the periodic density functional theory (DFT) method using Dmol3<sup>[3]</sup> module in Material Studio software package.<sup>[4]</sup> The initial configuration was fully optimized by Perdew-Wang (PW91)<sup>[5]</sup> generalized gradient approximation (GGA) method with the double numerical basis sets plus polarization function (DNP). The core electrons for metals were treated by effective core potentials (ECP). The self-consistent field (SCF) converged criterion was within  $1.0 \times 10^{-5}$  hartree atom<sup>-1</sup> and the converging criterion of the structure optimization was  $1.0 \times 10^{-3}$  hartree bohr<sup>-1</sup>. The Brillouin zone is sampled by  $1 \times 1 \times 1$   $k$ -points, and test calculations reveal that the increase of  $k$ -points does not affect the results.

## B. Supporting Figures

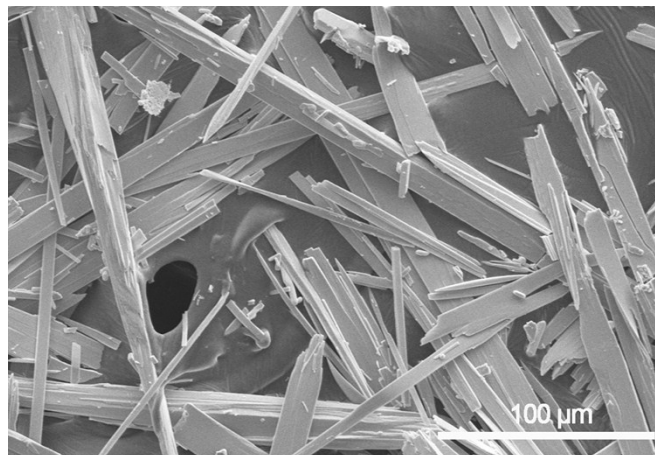


**Figure S1.** SEM image of the as-prepared OIHP-AD crystals synthesized under hydrothermal condition.

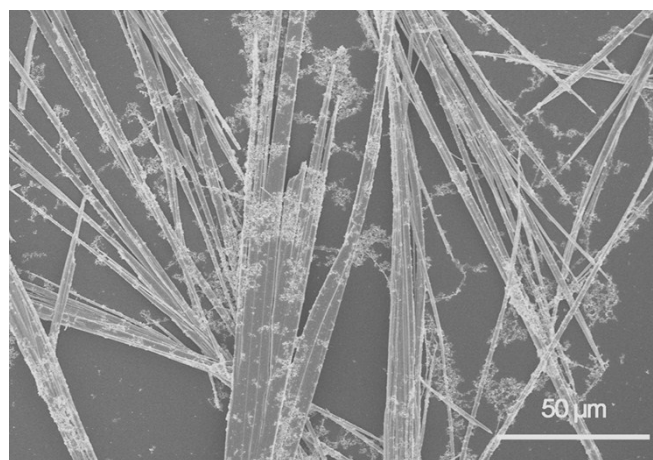


**Figure S2.** SEM image of the as-prepared OIHP-AD crystals synthesized in aqueous solution at room temperature.

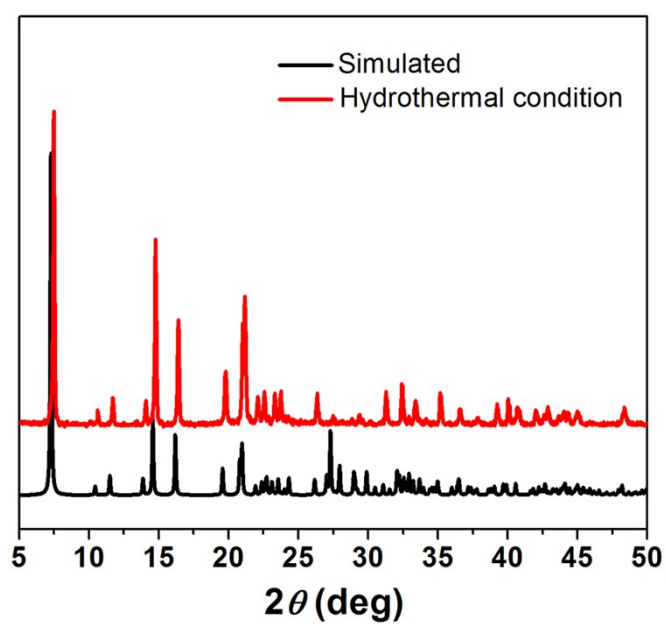


**Figure S3.** PXRD patterns of simulated (black) and experiment OIHP-AD (red) synthesized under hydrothermal condition.

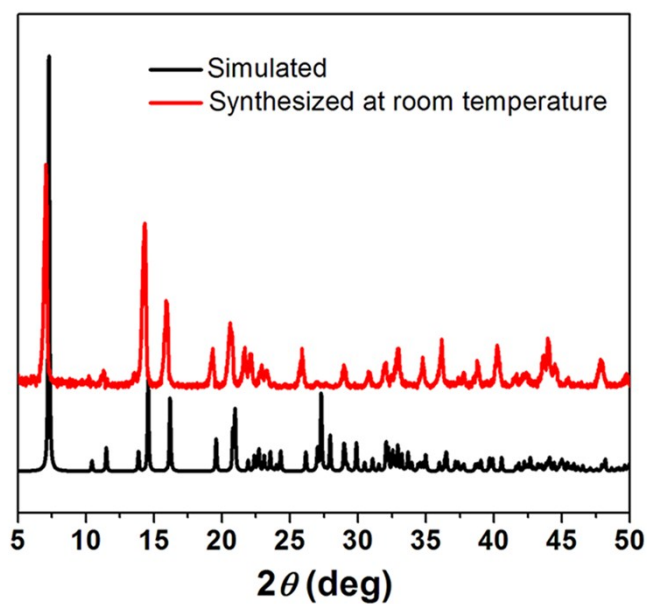


**Figure S4.** PXRD patterns of simulated (black) and experiment OIHP-AD (red) synthesized in aqueous solution at room temperature.

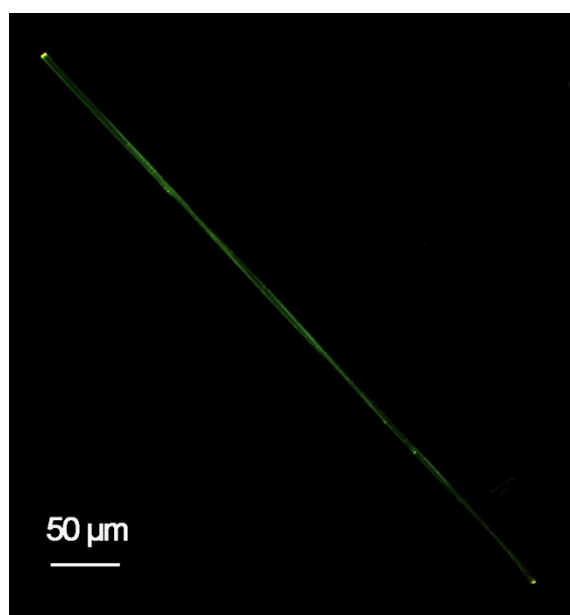


**Figure S5.** Photoluminescence microscope image of single OIHP-AD micro-belt.

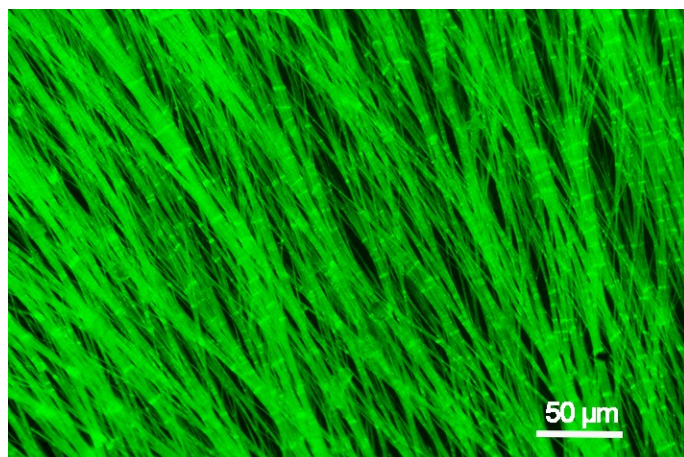
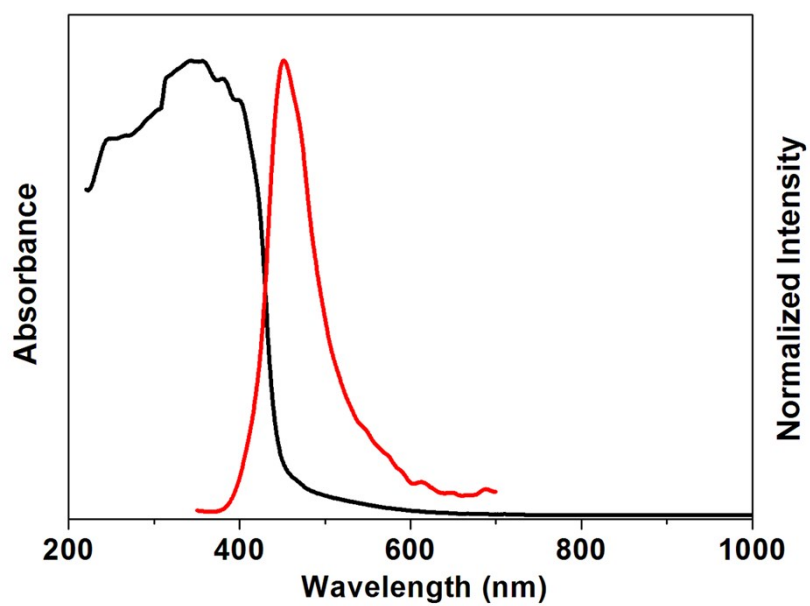
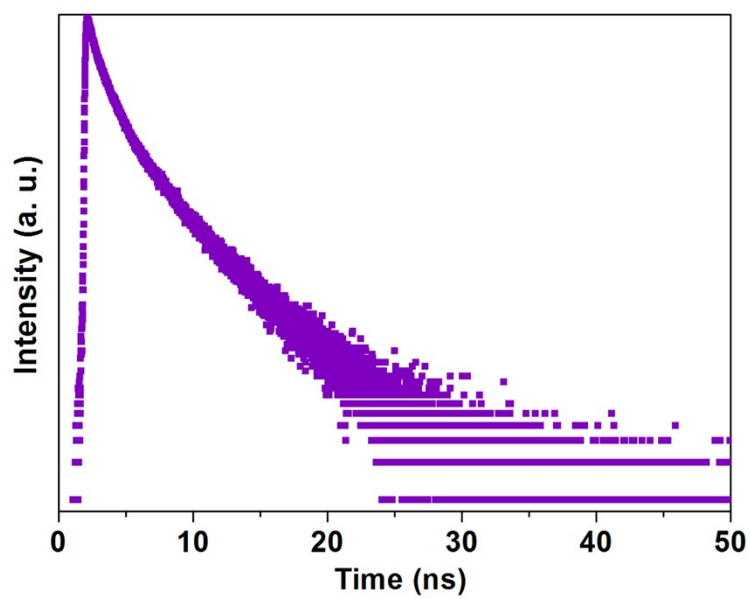


**Figure S6.** Photoluminescence microscope images of OIHP-AD self-supporting film.



(a)



(b)

**Figure S7.** (a) UV-vis absorption (black) and fluorescence emission spectrum (red, excitation at 280 nm) of AD in solid state at room temperature. (b) Time-resolved fluorescence decay of AD in solid.



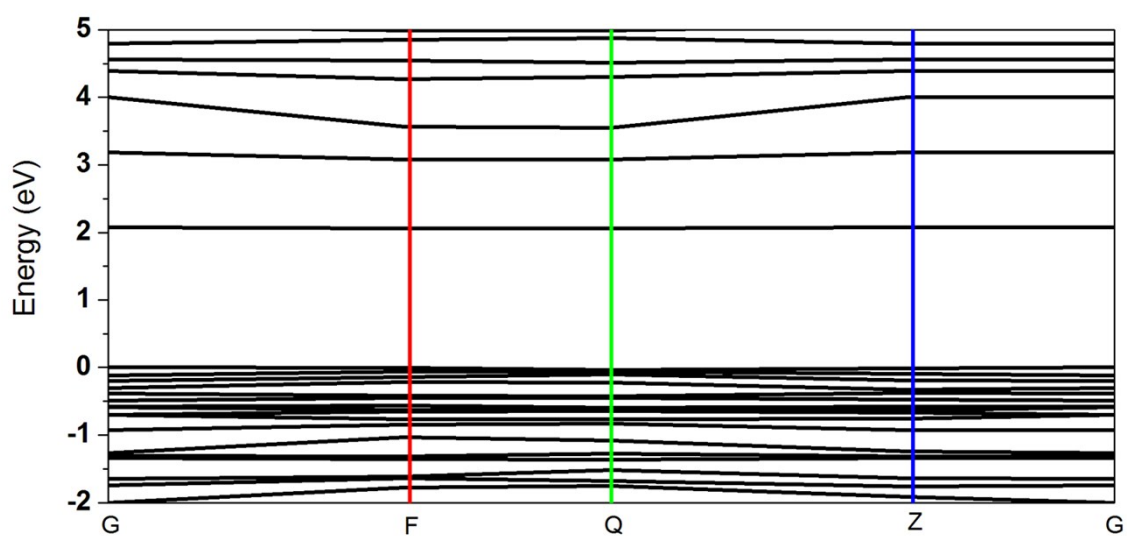


**Figure S8.** Calculated energy band structure of OIHP-AD.

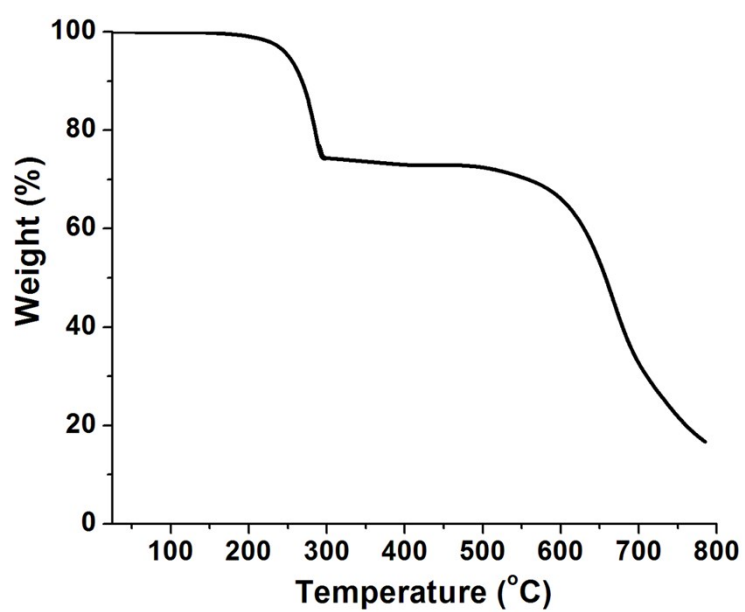
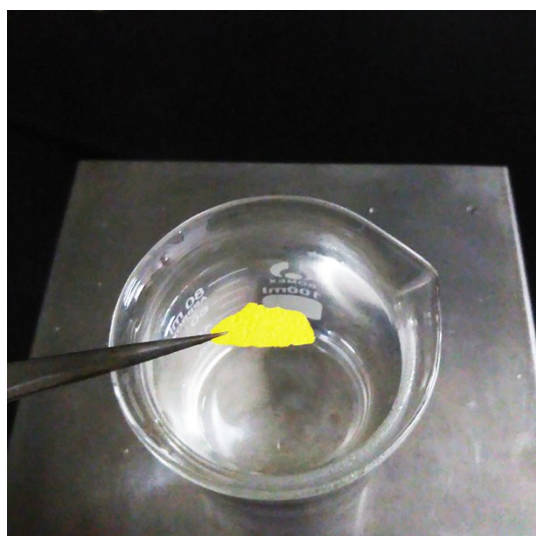
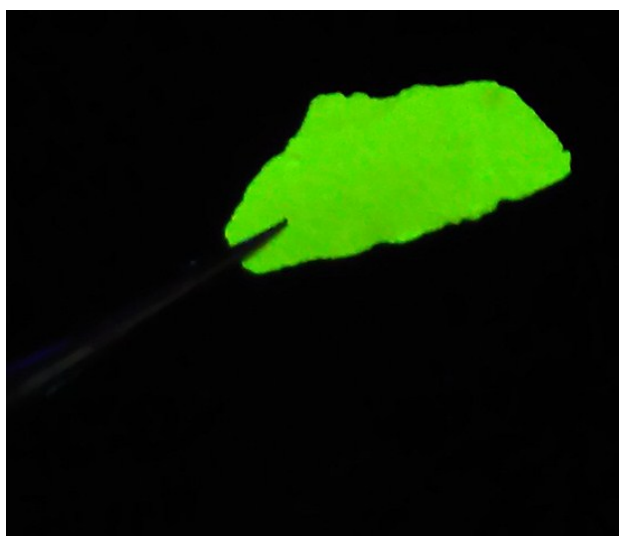


**Figure S9.** Thermogravimetric analysis (TGA) curves of OIHP-AD crystals.



(a)



(b)

**Figure S10.** (a) Photographs of OIHP-AD self-supporting film exposed to steam for 24 h and (b) further radiated under UV (365 nm) light.

## C. Supporting Tables

**Table S1.** Crystallographic data for OIHP-AD.

Samples	OIHP-AD
Chemical formula	$C_{6.5}H_5N_{0.5}Cl_{2.5}Pb$
Formula weight	386.96
Crystal system	Triclinic
Space group	$P\bar{1}$
$a$ (Å)	4.0291(3)
$b$ (Å)	8.8371(6)
$c$ (Å)	12.3963(10)
$\alpha$ (°)	100.672(6)
$\beta$ (°)	91.860(6)
$\gamma$ (°)	102.273(6)
$V$ (Å <sup>3</sup> )	422.64(5)
$Z$	2
$D$ (g cm <sup>-3</sup> )	3.0404
$\mu$ (mm <sup>-1</sup> )	20.678
$T$ (K)	296(2)
$R_{\text{int}}$	0.0720
Goof	0.943
$R_1$ ( $I > 2\sigma(I)$ )	0.0477
$wR_2$ ( $I > 2\sigma(I)$ )	0.0549

$$R_1 = \Sigma||F_o| - |F_c||/\Sigma|F_o|, wR_2 = [\Sigma w(F_o^2 - F_c^2)^2/\Sigma w(F_o^2)^2]^{1/2}$$

## D. Supporting References

- [1] CrysAlisPro, Rigaku Oxford Diffraction, Version 1.171.39.6a.
- [2] G. M. Sheldrick, *Acta Crystallogr. Sect. A*. 2008, **64**, 112.
- [3]. a) B. Delley, *J. Chem. Phys.* 1990, **92**, 508; b) B. Delley, *J. Chem. Phys.* 2000, **113**, 7756.
- [4] Dmol3 Module, MS Modeling, Version 2.2; Accelrys Inc.: San, Diego, 2003.
- [5] J. P. Perdew, J. A. Chevary, S. H. Vosko, K. A. Jackson, M. R. Pederson, D. J. Singh, C. Fiolhais, *Phys. Rev. B*. 1992, **46**, 6671.